Antigen-specific Vγ2Vδ2 T effector cells confer homeostatic protection against pneumonic plaque lesions

Dan Huang[a], Crystal Y. Chen[a], Zahida Ali[a], Lingyun Shao[a], Ling Shen[b], Hank A. Lockman[c], Roy E. Barnewall[c], Carol Sabourin[c], James Eestep[c], Armin Reichenberg[d], Martin Hintz[d], Hassan Jomaa[d], Richard Wang[a], and Zheng W. Chen[a,1]

[a]Department of Microbiology and Immunology, Center for Primate Biomedical Research, University of Illinois College of Medicine, Chicago, IL 60612; [b]Department of Medicine, Beth Israel Deaconess Medical Center, Boston, MA 02215; [c]Battelle Medical Research/Evaluation Facility, Battelle Memorial Institute, Columbus, OH 43201; and [d]Institut für Klinische Immunologie und Transfusionsmedizin, Justus-Liebig-Universität Giessen, Langhansstrasse 7, 35392 Giessen, Germany

Edited by Jack F. Bukowski, Boston, MA, and accepted by the Editorial Board March 20, 2009 (received for review November 6, 2008)

The possibility that Vγ2Vδ2 T effector cells can confer protection against pulmonary infectious diseases has not been tested. We have recently demonstrated that single-dose (*E*)-4-hydroxy-3-methyl-but-2-enyl pyrophosphate (HMBPP) plus IL-2 treatment can induce prolonged accumulation of Vγ2Vδ2 T effector cells in lungs. Here, we show that a delayed HMBPP/IL-2 administration after inhalational *Yersinia pestis* infection induced marked expansion of Vγ2Vδ2 T cells but failed to control extracellular plague bacterial replication/infection. Surprisingly, despite the absence of infection control, expansion of Vγ2Vδ2 T cells after HMBPP/IL-2 treatment led to the attenuation of inhalation plague lesions in lungs. Consistently, HMBPP-activated Vγ2Vδ2 T cells accumulated and localized in pulmonary interstitials surrounding small blood vessels and airway mucosa in the lung tissues with no or mild plague lesions. These infiltrating Vγ2Vδ2 T cells produced FGF-7, a homeostatic mediator against tissue damages. In contrast, control macaques treated with glucose plus IL-2 or glucose alone exhibited severe hemorrhages and necrosis in most lung lobes, with no or very few Vγ2Vδ2 T cells detectable in lung tissues. The findings are consist with the paradigm that circulating Vγ2Vδ2 T cells can traffic to lungs for homeostatic protection against tissue damages in infection.

(*E*)-4-hydroxy-3-methyl-but-2-enyl pyrophosphate immunotherapeutics | lung | macaques | immune regulation | clonal expansion

Accumulating evidence suggests that human Vγ2Vδ2 (also called Vγ9Vδ2) T cells may play a role in mediating immunity against microbial pathogens (1–8). Vγ2Vδ2 T cells constitute 60–95% of circulating human γδ T cells and are unique in their ability to massively expand during various bacterial and protozoal infections (9). Vγ2Vδ2 T cell expansion appears to be specifically mediated by certain low molecular weight foreign- and self-nonpeptidic phosphorylated metabolites of isoprenoid biosynthesis [e.g., (*E*)-4-hydroxy-3-methyl-but-2-enyl pyrophosphate (HMBPP), isopentenyl pyrophosphate, and its isomer dimethylallyl pyrophosphate] (10–12). HMBPP is produced in the newly-discovered 2-C-methyl-D-erythritol-4-phosphate pathway of isoprenoid biosynthesis of most eubacteria, apicomplexan protozoa, plant chloroplasts, and algae but not in vertebrates and thus normally not in the human host (13). We have recently demonstrated that HMBPP is associated with antigen-presenting cells and specifically recognized by Vγ2Vδ2 T cell receptor (TCR) (14). We have also shown that single-dose HMBPP treatment plus IL-2 can induce remarkable expansion of Vγ2Vδ2 T cells in the blood and prolonged accumulation of Vγ2Vδ2 T cells in lungs in nonhuman primates (15–17). Vγ2Vδ2 T cells accumulating in lungs can re-recognize HMBPP and mount effector function of production of antimicrobial cytokines, IFN-γ, and perforin/granzyme B (17, 18). In fact, rapid recall-like expansion of pulmonary Vγ2Vδ2 T cells after *Mycobacterium tuberculosis* infection of bacillus Calmette–Guérin-vaccinated juvenile rhesus macaques correlates with protection against early fatal tuberculosis (1).

Yersinia pestis is one of the world's most virulent human pathogens. Inhalation of this Gram-negative bacterium causes pneumonic plague, a rapidly-progressing and usually fatal disease. The worldwide storage of *Y. pestis* at many laboratories and the existence of extensively antibiotic-resistant *Y. pestis* strains have made the plague bacilli a potentially-devastating terrorism and warfare agent (19). Protective immune responses against fatal inhalation plague remain incompletely understood. In fact, F1/LcrV-based vaccines protect mice and cynomolgus macaques but do not effectively confer protection in African green monkeys (19–21). Elucidating innate and adaptive immune responses in the settings of vaccination and immune intervention will facilitate ultimate development of antiplague vaccines and immunotherapeutics.

The possibility that Vγ2Vδ2 T effector cells accumulating in lungs after HMBPP/IL-2 administration can confer therapeutic effect on pulmonary infectious diseases, including inhalation plague, has not been tested. Interestingly, *Y. pestis* carries the gene encoding hydroxymethylbutenyl 4-diphosphate synthase (also called GcpE) involved in production of phosphoantigen HMBPP recognized by Vγ2Vδ2 T cells (12). In fact, the *Y. pestis* antigen fraction containing nonpeptide small molecules can stimulate expansion of Vγ2Vδ2 T cells. This finding adds to the rationale for studies of Vγ2Vδ2 T cells and their potential antiplague immune function during inhalational *Y. pestis* infection. Becausethe cynomolgus macaque model of *Y. pestis* infection has proven to be useful for evaluating vaccines against pneumonic plague (20, 21), we used this plague model to undertake a proof-of-concept study examining a potential role of Vγ2Vδ2 T cells in immunity against an extracellular *Y. pestis* bacilli infection. In this context, we sought to determine whether a delayed HMBPP/IL-2 treatment regimen after inhalational *Y. pestis* infection could induce activation/expansion of Vγ2Vδ2 T cells and confer protection against inhalation plague in the macaque model. We found that a delayed HMBPP/IL-2 treatment induced marked expansion of Vγ2Vδ2 T cells but failed to control *Y. pestis* replication and dissemination. Surprisingly, however, expansion of Vγ2Vδ2 T cells after the delayed HMBPP/IL-2 treatment led to the apparent attenuation of plague lesions in lungs. HMBPP-activated Vγ2Vδ2 T cells accu-

Author contributions: D.H., C.Y.C., and Z.W.C. designed research; D.H., C.Y.C., Z.A., L. Shao, L. Shen, H.A.L., R.E.B., C.S., J.E., and R.W. performed research; A.R., M.H., and H.J. contributed new reagents/analytic tools; D.H., C.Y.C., and Z.W.C. analyzed data; and Z.W.C. wrote the paper.

The authors declare no conflict of interest.

This article is a PNAS Direct Submission. J.F.B. is a guest editor invited by the Editorial Board.

[1]To whom correspondence should be addressed. E-mail: zchen@uic.edu.

This article contains supporting information online at www.pnas.org/cgi/content/full/0811250106/DCSupplemental.

MEDICAL SCIENCES

Table 1. Outcomes of HMBPP/IL-2-treated and control monkeys after inhalational *Y. pestis* infection

Animal	Treatment	Sex	Inhaled cfu	Day of death
22744	HMBPP + IL-2	Female	364	N/A*
22739	HMBPP + IL-2	Female	69	8
22734	HMBPP + IL-2	Female	678	N/A*
22742	HMBPP + IL-2	Female	143	9
22802	HMBPP + IL-2	Male	319	6
22801	HMBPP + IL-2	Male	231	5
22746	Glucose + IL-2	Female	154	5
22749	Glucose + IL-2	Female	181	6
22811	Glucose + IL-2	Male	485	10
22748	Glucose	Female	328	N/A†
22735	Glucose	Female	347	8
22798	Glucose	Male	207	6

N/A, not available.
*Necropsy showed no lesions.
†Necropsy showed plague lesions in lungs.

mulated and localized in pulmonary interstitials surrounding small blood vessels and airway mucosa in the lung tissues with no or mild plague lesions. The findings are consistent with the paradigm that circulating Vγ2Vδ2 T cells can traffic to lungs for homeostatic protection against tissue damages in infection.

Results

Delayed Treatment of Macaques with Single-Dose HMBPP Plus IL-2 Induced Marked Expansion of Vγ2Vδ2 T Cells During Inhalational *Y. pestis* Infection. Because inhalational plague can progress rapidly, we sought to determine whether early activation of Vγ2Vδ2 T cells by HMBPP/IL-2 treatment can enhance immune responses and confer attenuation of pneumonic plague in cynomolgus monkeys. We presume that a 5-h delay after inhalational *Y. pestis* infection would be a practical time point in which to determine whether HMBPP/IL-2 treatment could induce activation of Vγ2Vδ2 T cells and attenuation of inhalation plague. Thus, 12 cynomolgus macaques were infected with *Y. pestis* by aerosol using the head-only challenging system as described (1, 22). Five hours after the inhalational *Y. pestis* infection, 6 macaques were treated with single-dose (50 mg/kg) HMBPP plus IL-2 treatment (17); 6 other animals were treated as controls with glucose plus IL-2 or glucose only (Table 1). HMBPP/IL-2 treatment consistently induced major expansion of Vγ2Vδ2 T cells during inhalational *Y. pestis* infection. Vγ2Vδ2 T cells in the test group expanded and accounted for mean 48% of total T cells in the blood circulation at 5 days after the inhalational *Y. pestis* infection and HMBPP/IL-2 treatment (Fig. 1*A*). Consistently, absolute mean numbers of Vγ2Vδ2 T cells on day 5 after HMBPP/IL-2 treatment increased to mean 8,500 per μL in the blood circulation (Fig. 1*B*). The surviving macaques showed either a sustained 10-fold expansion of Vγ2Vδ2 T cells or a return to baseline at weeks 2, 3, and 4 after the treatment/infection.

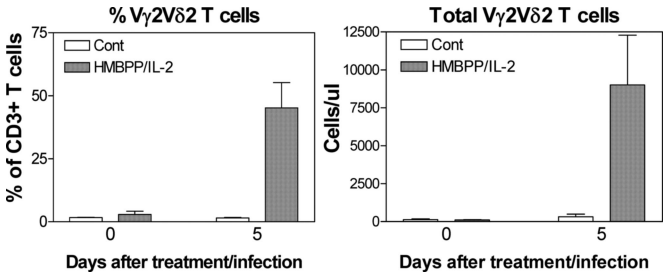

Fig. 1. The delayed treatment of macaques with single-dose HMBPP plus IL-2 induced marked expansion of Vγ2Vδ2 T cells during inhalational *Y. pestis* infection. Shown are percentage (*Left*) and absolute numbers (*Right*) of Vγ2Vδ2 T cells in blood circulation before and after inhalational *Y. pestis* infection. Data are mean values with SEM error bars of 6 macaques for each group.

Delayed HMBPP/IL-2 Treatment Regimen Did Not Control *Y. pestis* Replication in Lungs, Rapid Extra-Thoracic Dissemination, or Fatal Inhalation Plague. Although the delayed HMBPP/IL-2 treatment induced major expansion of Vγ2Vδ2 T cells, inhalation of large-dose virulent *Y. pestis* bacteria resulted in rapidly fatal pneumonic plague. Only 2 of 6 macaques treated with HMBPP/IL-2 survived the fatal inhalation plague during 1-month follow-up; 4 other cotreated macaques were dying from circulation collapse or distressed breathing at days 5–10 after the infection. All control monkeys treated with glucose/IL-2 were dying or moribund 7–10 days after inhalational *Y. pestis* infection; 2 of 3 monkeys treated with glucose alone also suffered from the rapidly fatal inhalation plague (Table 1). There was no statistical difference in survival between the HMBPP/IL-2 treated group and control group. Notably, the clinical moribund or death appeared to be linked to the severe septicemia caused by rapid extra-thoracic dissemination of *Y. pestis* infection, because all dying monkeys had extremely large numbers of *Y. pestis* bacteria in blood and suffered from the septicemia-related circulation collapse (Table S1). All moribund animals regardless of treatments also exhibited extremely-high levels of bacterial burdens in lung homogenates (Table S1). Thus, expansion of Vγ2Vδ2 T cells after the delayed HMBPP/IL-2 treatment did not confer immune control of *Y. pestis* replication or fatal inhalation plague, which was characterized microbially by high bacterial burdens in lungs and rapid extra-thoracic dissemination to the blood stream.

Expansion of Vγ2Vδ2 T Cells After the Delayed HMBPP/IL-2 Treatment Resulted In Attenuation of Inhalation Plague Lesions After Pulmonary Infection with Large-Dose *Y. pestis*. Surprisingly, although the delayed HMBPP/IL-2 treatment did not confer clinical protection against inhalational *Y. pestis* infection, expansion of Vγ2Vδ2 T cells after the treatment resulted in an apparent attenuation of inhalation plague lesions in lungs. Necropsy studies done between 1 and 4 weeks indicated that the control macaques developed apparent hemorrhages or severe hemorrhages in lungs, mostly involving the whole or half lobe for all 6 lung lobes (Fig. 2, Figs. S1 and S2, and Table 2). Even for the single control survival macaque with subclinical plague, unresolved hemorrhages were still evident in 2 lobes at day 28. (Fig. 2 and Table 2). In contrast, the HMBPP-treated macaques displayed no or relatively-focal plague lesions in lungs compared with those in control animals (Fig. 2, Figs. S1 and S2, and Table 2). Even though 4 of 6 HMBPP/IL-2-treated macaques were dying from high bacterial burden and severe septicemia, only 2 of the HMBPP/IL-2-treated macaques had 1 lobe displaying extensive involvement of hemorrhages (Fig. 2, Figs. S1 and S2, and Table 2). Hemorrhagic lesions in these 4 animals usually involved only 1/4–1/2 lobe or less in 2 lungs (Fig. 2, Figs. S1 and S2, and Table 2). Those 2 survival macaques exhibited almost "normal" lungs at the time the necropsy was done (Fig. 2 and Table 2).

To compare lung plague lesions between HMBPP/IL-2-treated and control groups, a scoring system for lung pathologic involvements was adopted from previous nonhuman primate studies (23, 24). The plague lesion scores calculated from HMBPP/IL-2-treated macaques were much lower than those of the animals in the control groups ($P < 0.001$; Table 2).

Histology analyses also supported what were seen in gross pathology studies at necropsy. Overall, no apparent hemorrhages, necrosis, or damages of pulmonary structures were seen in the lung lobes with no or mild gross hemorrhages of HMBPP/IL-2-treated monkeys, although there were vasodilatation and congestion in venules in pulmonary mucosa (Fig. 3). In the tissue sections from gross hemorrhage lobes, alveoli were filled with red blood cells, lymphocytes, or inflammatory cells and edema fluid, and they were associated with congested capillaries and venules (Fig. 3). Impor-

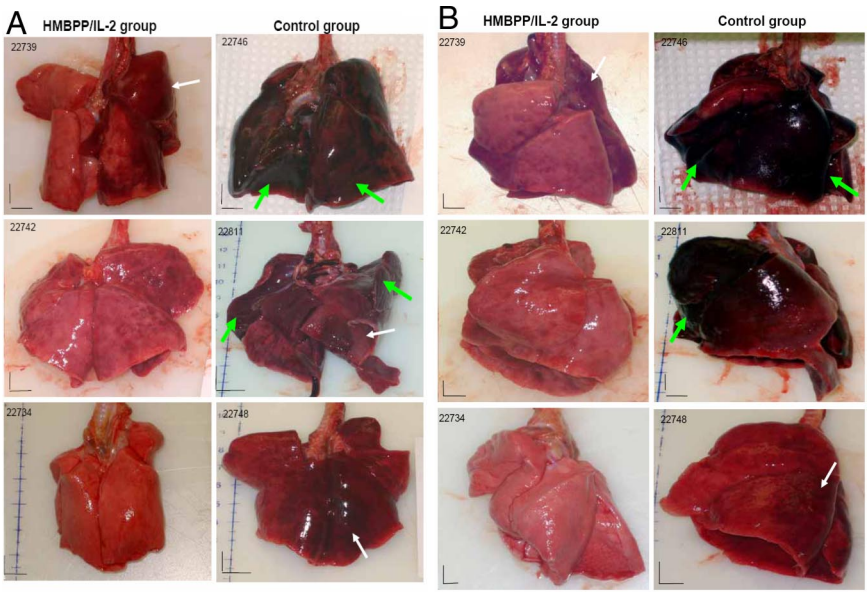

Fig. 2. Expansion of Vγ2Vδ2 T cells after the delayed HMBPP/IL-2 treatment resulted in apparent attenuation of pneumonic plague lesions at gross pathology level after pulmonary infection with large-dose *Y. pestis*. (*A*) Front/back-view pictures show comparisons of representative gross pathology between HMBPP/IL-2 treated (*Left*) and control (*Right*) monkeys. The control monkeys displayed hemorrhagic outlook (illustrated by a white arrow) or severe hemorrhages (illustrated by large green arrows) in most lung lobes. HMBPP/IL-2 treated monkeys exhibited relatively focal hemorrhages in limited numbers of lobes or no hemorrhages.(*Middle* and *Bottom*) Shown is the gross pathology for the lungs of the 2 survival monkeys. Note that the representative HMBPP/IL-2-treated monkey (22734) showed no hemorrhages or other lesions in the lung, whereas the glucose-treated control animal (22748) still displayed unresolved hemorrhagic changes, which was consistent with histology alteration seen under microscope (Fig. 3*B*). Similar gross pathology was seen in other 6 monkeys (Fig. S1). (*B*) The side-view pictures show gross pathology comparisons for the same 6 monkeys from HMBPP/IL-2-treated (*Left*) and control (*Right*) groups. The gross pathologic changes on the side view were consistent with those on the front view. Similar changes were seen in 6 other monkeys (Fig. S2). The vertical and horizontal bars are 1-cm scale calculated from the digital rulers in the photos.

tantly, many lymphocytes infiltrated in the interstitials surrounding intact arterioles, bronchial mucosa, and alveoli in the HMBPP/IL-2-treated monkeys. In contrast, hemorrhages and necrosis were seen in the tissue sections prepared from the lung lobes with severe gross hemorrhages of control monkeys treated with glucose or glucose plus IL-2 (Fig. 3). Hemorrhages were seen in the wall of large blood vessels, which appeared to contribute to extensive hemorrhages (Fig. 3). Hemorrhages also occurred in the lung tissues and small vessels, which were associated with extensive necrosis and infiltration with polymorphs, neutrophils, and macrophages in the lung lobes with severe gross hemorrhages. Vessels and their neighbor pulmonary tissues were even destroyed in the lung lobes with severe gross hemorrhages (Fig. 3). Even for the single control survival macaque with subclinical plague, changes in unresolved hemorrhages were still evident (Fig. S3).

Collectively, these results demonstrated that expansion of Vγ2Vδ2 T cells after HMBPP/IL-2 treatment led to apparent attenuation of inhalation plague lesions after pulmonary infection with large-dose *Y. pestis*.

HMBPP-Activated Vγ2Vδ2 T Cells Accumulated and Localized in Pulmonary Interstitials Surrounding Blood Vessels and Airway Mucosa in the Lung Tissues with No or Wild Plague Lesions. Because no or mild plague lesions in HMBPP/IL-2-treated monkeys were associated with the expansion of Vγ2Vδ2 T cells and infiltration of many lymphocytes in the interstitials surrounding intact arterioles and airway mucosa, we sought to determine whether those lymphocytes infiltrating in the interstitials were comprised of Vγ2Vδ2 T cells. To this end, we undertook immunohistochemistry studies to examine whether accumulation or localization of Vγ2Vδ2 T cells in lung tissues was coincident with attenuated plague lesions in the monkeys treated with HMBPP/IL-2. Interestingly, Vγ2Vδ2 T cells were detected in the pulmonary interstitials in the lung tissues with no or mild plague hemorrhages or necrosis in the HMBPP/IL-2-treated macaques (Fig. 4 and Fig. S4). In fact, 3 patterns of accumulation and localization of Vγ2Vδ2 T cells were seen in the lung tissues with no or mild plague lesions: (*i*) Vγ2Vδ2 T cells localized in alveolar walls or interstitials surrounding small blood vessels (Fig. 4 *Top*); (*ii*) Vγ2Vδ2 T cells lined up around bronchiolar small veins and bronchiolar mucosa and in the peri-bronchiolar lymphoid follicles (Fig. 4 *Middle* and Fig. S4); and (*iii*) Vγ2Vδ2 T cells were present in the inflammatory exudates in the interstitial or alveolar, which might represent advanced inflammation (Fig. 4 *Bottom* and Fig. S4). These patterns of localization for Vγ2Vδ2 T cells appeared to implicate different levels of the cellular barriers for holding pulmonary vessels or airway mucosa from plague damages. Very few Vγ2Vδ2 T cells were detected in the tissues from the lung lobe with severe hemorrhages or necrosis of the monkey 20802, probably because of the nondelectability for damaged cells or tissues. In contrast, no or very few Vγ2Vδ2 T cells were detected in the lung tissue of control monkeys treated with glucose plus IL-2 or glucose alone. Thus, these results demonstrated that HMBPP-activated Vγ2Vδ2 T cells accumulated and localized in pulmonary interstitials surrounding blood vessels and airway mucosa in the lung tissues with no or mild plague lesions.

Vγ2Vδ2 T Effector Cells Around Blood Vessels or Airway Mucosa Produced the Tissue Homeostatic Factor, FGF-7, in Protective Lung Tissues. Finally, we sought to explore a potential mechanism by which Vγ2Vδ2 T effector cells conferred homeostatic protection against pneumonic plague lesions. Because murine skin γδ T cells capable of producing FGF-7 have been shown to play an important role in tissue homeostasis after tissue damage or inflammation (25), we undertook mechanistic studies to examine whether Vγ2Vδ2 T cells trafficking to lungs could produce FGF-7, which might contribute to the homeostatic protection. The immunohistochemistry studies showed that many Vγ2Vδ2 T cells distributing around lung

Table 2. Pathologic scores for plague lesions in HMBPP/IL-2-treated monkeys and control animals

Animal	Treatment	Day of death, postinfection	Pathologic score
22744	HMBPP + IL-2	NA	1
22739	HMBPP + IL-2	8	5
22734	HMBPP + IL-2	NA	0
22742	HMBPP + IL-2	9	5
22802	HMBPP + IL-2	6	15
22801	HMBPP + IL-2	5	5
22746	Glucose + IL-2	5	89
22749	Glucose + IL-2	6	28
22811	Glucose + IL-2	10	68
22748	Glucose	NA	12
22735	Glucose	8	75
22798	Glucose	6	24

NA, not available. $P = 0.007$ by t test (2 tails) for difference in plague lesion scores between HMBPP/IL-2 group (6 monkeys) and control group (6 monkeys). $P = 0.002$ by t test (2-tail) between HMBPP/IL-2 group (6 monkeys) and glucose/IL-2 group (3 monkeys). $P = 0.02$ by ANOVA (2-way) between HMBPP/IL-2 group (6 monkeys) and control group (6 monkeys).

vessels or airway mucosa were able to produce FGF-7 (Fig. 5). In vitro studies also showed that HMBPP/IL-2 stimulation of Vγ2Vδ2 T cells resulted in production of FGF-7 by these γδ T cells. This mechanistic finding implicates a potential mechanism underlying the attenuation of plague hemorrhages or necrosis by Vγ2Vδ2 T effector cells.

Discussion

It is not totally unexpected that the delayed HMBPP/IL-2 treatment regimen conferred no therapeutic effect on *Y. pestis* replication, rapid extra-thoracic dissemination, and fatal inhalation plague. *Y. pestis* is an extremely virulent extracellular pathogen capable of inducing fatal infection in mammals. One would expect that neutralizing antibodies might more efficiently control extracellular *Y. pestis* replication than Vγ2Vδ2 T cells, although the Vγ2Vδ2 T cells can produce bactericidal protein, granulysin, and some other antimicrobial cytokines (18). An earlier study (2) showed that transfused Vγ2Vδ2 T cells in hu-SCID mice mediate resistance to experimental systemic infections with extracellular bacteria such as *Staphylococcus aureus* and *Escherichia. coli*. The pulse-cytokine-production effect of Vγ2Vδ2 T cells may contribute to control of those bacteria in the hu-SCID mouse model system. Other microbial and host factors that distinguish hu-SCID mice from monkeys might also be the explanations for the finding in hu-SCID mice. It is noteworthy that our proof-of-concept studies were undertaken with large-dose *Y. pestis* inoculums for inhalational infection of macaques, and such overwhelming bacterial burden may be quite difficult to control.

The current study demonstrates that expansion of Vγ2Vδ2 T cells after the delayed HMBPP/IL-2 treatment can confer homeostatic protection against inhalation plague lesions. The extensive pathology evaluation demonstrates that the delayed HMBPP/IL-2 treatment after inhalational *Y. pestis* infection induces marked expansion of Vγ2Vδ2 T cells and leads to apparent attenuation of inhalation plague lesions in lungs. There are quite significant differences in plague hemorrhages between the HMBPP/IL-2-treated group and control group. The results appear to represent a novel observation because such homeostatic protection against plague lesions does not depend on the control of *Y. pestis* replication. Vγ2Vδ2 T cells seem to exert antiinflammation effects rather than control plague bacterial replication or infection. These results appear to differ somehow from the murine γδ T cell-mediated reduction of bacterial loads in γδ KO mice, although γδ T cell deficiency can lead to organ damage in sepsis (26). Another

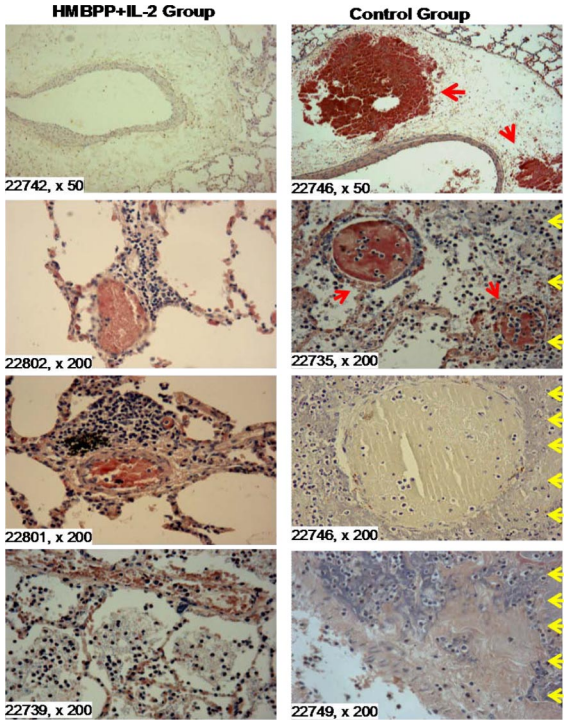

Fig. 3. Expansion of Vγ2Vδ2 T cells after the delayed HMBPP/IL-2 treatment resulted in apparent attenuation of pneumonic plague lesions at histology level after pulmonary infection with large-dose *Y. pestis*. Shown is histology evaluating lung tissue sections of moribund HMBPP/IL-2-treated macaques (*Left*) and moribund control animals (*Right*). H&E-stained sections were taken from 6 representative dying macaques, 3 for each group, with macaque ID and magnification indicated for each image. No apparent hemorrhages or damages of alveoli were seen in the lung lobes with no or mild gross hemorrhages of the representative HMBPP/IL-2-treated monkeys (20801 and 20802), despite vasodilatation and congestion in venules in bronchial mucosa and lymphoid follicles. In the tissue sections from gross hemorrhage lobes as pointed by a white arrow in Fig. 2*A* for the monkey 22739, alveoli were filled with red blood cells, lymphocytes, or inflammatory cells and edema fluid and associated with congested capillaries and venules. Note that many lymphocytes infiltrated in the interstitials surrounding intact arterioles (22802 and 22801) and bronchial mucosa and alveoli in the HMBPP/IL-2-treated monkeys (22802, 22801, and 22739). In contrast, control monkeys treated with glucose plus IL-2 or glucose alone displayed hemorrhagic and necrotic histology in the lung lobes with severe gross hemorrhages. Note that hemorrhages occurred in the wall of large blood vessels (large red arrows, 22746), which led to thinning, degeneration, or necrosis in the tunica media and tunica adventitia of the vessel (22746). Hemorrhages also occurred in the lung tissues (red blood cells) and small vessels (small red arrows, 27235), which were associated with extensive necrosis (yellow arrows) and infiltration with polymorphs neutrophils and macrophages in the lung lobes with severe gross hemorrhages (illustrated in the section of 22735, 22746, and 22749). Vessels and their neighbor pulmonary tissues were even destroyed in the lung lobes with severe gross hemorrhages (illustrated in the section of 22749). Similar changes were seen in other monkeys. Of note, the lung lobes with severe gross hemorrhages from the control monkeys and the HMBPP/IL-2-treated animal (20802) showed similar necrotic changes.

interesting aspect is that Ag-specific Vγ2Vδ2 T cells expand in the circulation, but are able to traffic to lungs for homeostatic protection against plague lesions. Because HMBPP phosphoantigen is produced by a variety of pathogens, activation of Vγ2Vδ2 T cells in those microbial infections may contribute to homeostatic protection against tissue damages during infections.

Vγ2Vδ2 T cells accumulating and localizing in lung tissues after HMBPP/IL-2 treatment appear to contribute to homeostatic protection or attenuation of plague lesions after inhalational *Y. pestis* infection. Vγ2Vδ2 T cells may help to prevent or reduce plague *Y. pestis*-mediated damage of blood vessels or vascular endothelial

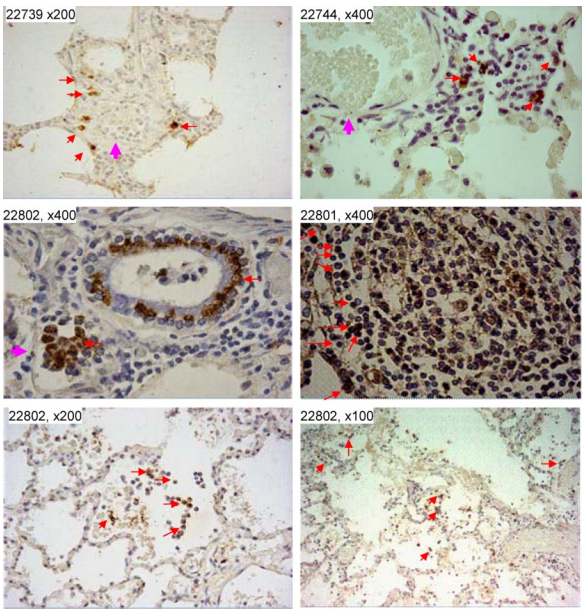

Fig. 4. Vγ2Vδ2 T cells were present in the lung tissues with no or mild plague hemorrhages/necrosis in the HMBPP/IL-2-treated macaques. (*Top*) Vγ2Vδ2 T cells localized in alveolar walls or interstitials surrounding small blood vessels. (*Middle*) Vγ2Vδ2 T cells lined up around bronchiolar small veins and the bronchiolar airways and in the peri-bronchiolar lymphoid follicles. (*Bottom*) Vγ2Vδ2 T cells accumulated in the inflammatory exudates in the interstitial or alveolar. Note that Vγ2Vδ2 T cells were present in the absence of apparent hemorrhages or necrosis. Red arrows point to positively-stained Vγ2Vδ2 T cells; pink arrows point to the vessels. The 3 patterns of Vγ2Vδ2 T cells' localization were also seen in other HMBPP/IL-2-treated monkeys (Fig. S3). No Vγ2Vδ2 T cells were detected in lung tissues from control monkeys treated with glucose plus IL-2 or glucose alone (Fig. S3). Vγ2Vδ2 T cells are not detectable in lung tissues of healthy uninfected macaques (22).

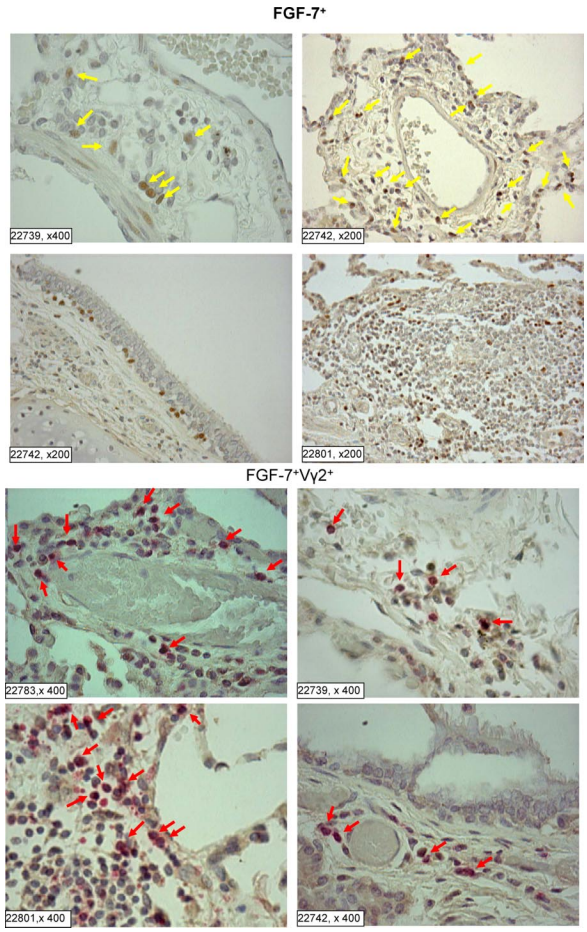

Fig. 5. Vγ2Vδ2 T cells distributing around lung vessels or airway mucosa were able to produce a tissue homeostatic factor, FGF-7. (*Upper*) The single-color staining sections showing many FGF-7 positive lymphocytes (brown, marked by yellow arrows) distributing around blood vessels (upper 2 photos), in the bronchus mucosa (lower left) and in the bronchial lymphoid follicles (lower right). (*Bottom*) The double staining sections of pulmonary mucosae. The lymphocytes coexpressing FGF-7 and Vγ2 TCR were stained dark red (indicated by red arrows). Note that almost all FGF-7-positive lymphocytes expressed Vγ2 TCR and localized in the lymphoid follicle (lower left, 22739) and around the vessels. Some cells were Vγ2 positive only (pink). Consistently, Vγ2Vδ2 T cells stimulated by HMBPP/IL-2 in culture were strongly positive for FGF-7. No FGF-7 was detectable in lung tissues of the control macaques.

cells. Our studies indicate that Vγ2Vδ2 T effector cells distributed around lung vessels or airway mucosa are able to produce FGF-7, a homeostatic cytokine against tissue damage/inflammation (25). This finding implies that local production of tissue homeostatic factor FGF-7 by Vγ2Vδ2 T cells may be one of the potential mechanisms by which Vγ2Vδ2 T cells confer homeostatic protection against plague lesions. In this context, Vγ2Vδ2 T cells may also induce production of damage-resistant or healing molecules by epithelial cells as described (27).

Thus, the delayed HMBPP/IL-2 treatment of macaques after inhalational *Y. pestis* infection induces remarkable expansion of Vγ2Vδ2 T cells and results in apparent attenuation of plague lesions in lung tissues. Because the delayed antibiotic treatment of inhalation plague is not highly successful for preventing plague death (19), a combination of antibiotics and Vγ2Vδ2 T cell-based intervention might have complementary effects on control of bacterial burdens and attenuation of plague lesions under some emergent conditions. Although this speculation needs to be investigated, the current study provides a paradigm that antigen-specific Vγ2Vδ2 T cells that expand in the circulation can traffic to pulmonary compartment for homeostatic protection against tissue damages or lesions in a pulmonary infection.

Methods

Macaque Animals and Inhalational *Y. pestis* Infection. A total of 12 cynomolgus monkeys, 4–8 years old, were included in these studies. All of the animal protocols for the studies were Institutional Animal Care and Use Committee-approved. The inhalational *Y. pestis* CO92 infection was done via a head-only inhalation system at the BSL-3 aerosol facility as described (1). Aerosolization of *Y. pestis* strain CO92 was developed for a head-only large-animal exposure system. By varying the concentration of *Y. pestis* in the Collison nebulizer, exposure concentrations of 10 to 5,000 cfu/L were generated. The atmosphere was sampled at 1 L/min through a low-pressure (7531) impinger containing PBS (without Mg or Ca) containing 0.01% gelatin (BSG) that was then analyzed by plating on tryptose agar. Based on a minute volume of ≈0.5 L/min for a macaque, a dosing range of 100 to 50,000 cfu of *Y. pestis* could be achieved in a 10- to 15-min exposure. Twelve Cynomolgus macaques (*Macaca fascicularis*) were randomized for order of challenge and assignment to study groups, with equal numbers of males and females in each group. The animals were exposed to an inhaled dose of 69–678 cfu over a period averaging 15 min.

Phosphoantigen HMBPP and IL-2 Administration. Five hours after inhalational *Y. pestis* infection, the test group of macaques received HMBPP plus IL-2 treatment; the control group of monkeys received either glucose plus IL-2 or glucose only. HMBPP was synthesized as described (28) with >98% purity (17). Immediately before injection HMBPP was reconstituted with saline and sterile-filtered. Recombinant human IL-2 (rhIL-2; Proleukin; Chiron) was reconstituted with sterile ddH_2O immediately before injection. Each macaque in the test group received a single 1-mL i.m. injection of 50 mg/kg HMBPP. These animals also received 0.5-mL s.c. injections of 1 million units of IL-2 once daily for 5 consecutive days beginning on the day of HMBPP treatment. For one control group, 50 mg/kg glucose was similarly given at on day 0. Another control group was given 50 mg/kg glucose plus1 million units of IL-2 once daily for 5 consecutive days.

Table 3. The criteria of score for evaluating gross hemorrhage involvement of lung lobes

Hemorrhage state	Rating	Score
No involvement of lobe	0	0
¼ or < ¼ of lobe involved	1	1
> ¼ - ½ of lobe involved	2	4
> ½-< entire lobe involved	3	9
Entire lobe involved	4	16

Immunofluorescent Staining and Flow Cytometric Analysis. For cell-surface staining, 100 μL of EDTA blood was treated with RBC Lysing Buffer (Sigma–Aldrich) and washed twice with 5% FBS–PBS before staining. Peripheral blood mononuclear cells were stained with up to 5 Abs [conjugated to FITC, phycoerythrin (PE), allophycocyanin, pacific blue and PE-Cy5 or allophycocyanin-Cy7] for at least 15 min. After staining, cells were fixed with 2% formaldehyde-PBS (Protocol Formalin) before analysis on a flow cytometer as described (17). The mouse mAbs used in the study have been described (17).

Bacterial CFU Counts. One milliliter of blood collected from each animal after inhalational *Y. pestis* infection was used to measure bacterial cfu. At necropsy, right and left middle lung lobes were randomly collected from each animal, and lung homogenate was generated by a homogenizer. One milliliter of blood or 15 mL of lung homogenate was serially diluted and plated on tryptose agar (Difco Laboratories).

Gross Pathologic Analyses of Pneumonic Plague Lesions and Scoring System. Complete necropsy was done for each of *Y. pestis*-infected monkeys as described (1, 22). Animals were killed by i.v. barbiturate overdose and immediately necropsied in a biological safety cabinet within a BSL-3 facility. Standard gross pathologic evaluation procedures were followed, with each step recorded and photographed. Multiple specimens including each lung lobes and other major organs were collected and labeled. Gross observations including, but not limited to, the presence, location, size, number, and distribution of lesions were recorded. Gross lesions were evaluated as hemorrhages and severe hemorrhages for each lobe of lungs and estimated as a percentage of the lobe involvement based on gross hemorrhagic outlooks from front-back and side views of organ exterior and cut surfaces. The gross plague lesions were evaluated and scored by using the published scoring systems as described (23, 24) (Table 3).

Microscopic Analyses of Pneumonic Plague Lesions. Lung tissues were fixed in buffered 10% formalin with ionized zinc (Z-Fix; Anatech). Histologic specimens were embedded in paraffin and sectioned at 5 μ for routine staining with H&E. The severity and extent of plague lesions for each lung lobe were examined by using digital scans of each lobe of lung to record total pixel counts of H&E-stained material, and specimen area was measured in square cm by using Image-Pro Plus software (MediaCybernetics) as described (22).

Immunohistochemistry Analysis of Vγ2Vδ2 T Cells in Tissues. Standard protocols for immunohistochemical analyses were used, as described (22), to evaluate Vγ2Vδ2 T cells in all tissue sections prepared from formalin-fixed lung lobes. The sections were treated for 5 min with 1% hydrogen peroxide in PBS to quench endogenous peroxidase, rinsed in PBS, and blocked for 10 min with protein block serum-free (Dako X0909) and rinsed in PBS. The sections were incubated with mouse anti-human Vγ2(Vγ9) 7B6 (from Marc Bonneville, Institut National de la Santé et de la Recherche Médicale, U601) in a concentration of 4.8 mg/mL for 1 h at room temperature and then incubated for 30 min with peroxidase-labeled polymer-conjugated goat anti-mouse immunoglobulins. The sections were rinsed in PBS after each incubation and then developed with 3,3′-diaminobenzidine chromogen solution as a substrate for 3–6 min and counterstained with Gill's Hematoxylin (Fisher Scientific) for 2 s. After dehydration in graded alcohols, sections were cleared in xylene and coverslipped.

For FGF-7 staining, deparaffinized slides were placed in target retrieval solution (Dako S3307) and heated for 1 min in a microwave. Twenty microliters of 15 μg/mL of goat anti-human KGF/FGF-7 Ab (R&D AF-251-VA) and peroxidase-labeled, polymer-conjugated rabbit anti-goat immunoglobulins (Dako P0160) were used for the staining, with diaminobenzidine as a substrate.

For FGF-7 and Vγ2 double staining, FGF-7 was stained as above, followed by Doublstain Block (Dako), and then stained for Vγ2 using 20 μL of 4.8 mg/mL of mouse anti-Vγ2 Ab (clone 7B6) and alkaline phosphatase-labeled polymer conjugated goat anti-mouse immunoglobulins (Dako K1395). Fast red was used as a substrate.

Statistical Analysis. Statistical analysis was done by using ANOVA and Student's *t* test as described (1).

ACKNOWLEDGMENTS. We thank members of Z.W.C.'s laboratory and C.S.'s group for technical assistance. This work was supported by National Institutes of Health Grants R01 HL64560, R01 RR13601, and U01 AI070426 (to Z.W.C.).

1. Shen Y, et al. (2002) Adaptive immune response of VγVδ2+ T cells during mycobacterial infections. *Science* 295:2255–2258.
2. Wang L, Kamath A, Das H, Li L, Bukowski JF (2001) Antibacterial effect of human Vγ2Vδ2 T cells in vivo. *J Clin Invest* 108:1349–1357.
3. Poccia F, et al. (1999) Phosphoantigen-reactive Vγ9Vδ2 T lymphocytes suppress in vitro human immunodeficiency virus type 1 replication by cell-released antiviral factors including CC chemokines. *J Infect Dis* 180:858–861.
4. Dieli F, et al. (2000) Vγ9/Vδ2 T lymphocytes reduce the viability of intracellular *Mycobacterium tuberculosis*. *Eur J Immunol* 30:1512–1519.
5. Ottones F, Dornand J, Naroeni A, Liautard JP, Favero J (2000) Vγ9Vδ2 T cells impair intracellular multiplication of *Brucella suis* in autologous monocytes through soluble factor release and contact-dependent cytotoxic effect. *J Immunol* 165:7133–7139.
6. Poccia F, et al. (2005) Antiviral reactivities of $\gamma\delta$ T cells. *Microbes Infect* 7:518–528.
7. Farouk SE, Mincheva-Nilsson L, Krensky AM, Dieli F, Troye-Blomberg M (2004) $\gamma\delta$ T cells inhibit in vitro growth of the asexual blood stages of *Plasmodium falciparum* by a granule exocytosis-dependent cytotoxic pathway that requires granulysin. *Eur J Immunol* 34:2248–2256.
8. Troye-Blomberg M, et al. (1999) Human $\gamma\delta$ T cells that inhibit the in vitro growth of the asexual blood stages of the *Plasmodium falciparum* parasite express cytolytic and proinflammatory molecules. *Scand J Immunol* 50:642–650.
9. Chen ZW, Letvin NL (2003) Vγ2Vδ2+ T cells and antimicrobial immune responses. *Microbes Infect* 5:491–498.
10. Hintz M, et al. (2001) Identification of (E)-4-hydroxy-3-methyl-but-2-enyl pyrophosphate as a major activator for human $\gamma\delta$ T cells in *Escherichia coli*. *FEBS Lett* 509:317–322.
11. Tanaka Y, et al. (1995) Natural and synthetic nonpeptide antigens recognized by human $\gamma\delta$ T cells. *Nature* 375:155–158.
12. Altincicek B, et al. (2001) Cutting edge: Human $\gamma\delta$ T cells are activated by intermediates of the 2-C-methyl-D-erythritol 4-phosphate pathway of isoprenoid biosynthesis. *J Immunol* 166:3655–3658.
13. Eberl M, et al. (2003) Microbial isoprenoid biosynthesis and human $\gamma\delta$ T cell activation. *FEBS Lett* 544:4–10.
14. Wei H, et al. (2008) Definition of APC presentation of phosphoantigen (E)-4-hydroxy-3-methyl-but-2-enyl pyrophosphate to Vγ2Vδ2 TCR. *J Immunol* 181:4798–4806.
15. Casetti R, et al. (2005) Drug-induced expansion and differentiation of Vγ9Vδ2 T cells in vivo: The role of exogenous IL-2. *J Immunol* 175:1593–1598.
16. Sicard H, et al. (2005) In vivo immunomanipulation of Vγ9Vδ2 T cells with a synthetic phosphoantigen in a preclinical nonhuman primate model. *J Immunol* 175:5471–5480.
17. Ali Z, et al. (2007) Prolonged (E)-4-hydroxy-3-methyl-but-2-enyl pyrophosphate-driven antimicrobial and cytotoxic responses of pulmonary and systemic Vγ2Vδ2 T cells in macaques. *J Immunol* 179:8287–8296.
18. Huang D, et al. (2007) Immune gene networks of mycobacterial vaccine-elicited cellular responses and immunity. *J Infect Dis* 195:55–69.
19. Smiley ST (2008) Immune defense against pneumonic plague. *Immunol Rev* 225:256–271.
20. Cornelius CA, et al. (2008) Immunization with recombinant V10 protects Cynomolgus macaques from lethal pneumonic plague. *Infect Immun* 76:5588–5597.
21. Mett V, et al. (2007) A plant-produced plague vaccine candidate confers protection to monkeys. *Vaccine* 25:3014–3017.
22. Huang D, et al. (2008) Immune distribution and localization of phosphoantigen-specific Vγ2Vδ2 T cells in lymphoid and nonlymphoid tissues in *Mycobacterium tuberculosis* infection. *Infect Immun* 76:426–436.
23. Good RC (1968) Biology of the mycobacterioses. Simian tuberculosis: Immunologic aspects. *Ann NY Acad Sci* 154:200–213.
24. Lin PL, et al. (2006) Early events in *Mycobacterium tuberculosis* infection in cynomolgus macaques. *Infect Immun* 74:3790–3803.
25. Jameson J, et al. (2002) A role for skin $\gamma\delta$ T cells in wound repair. *Science* 296:747–749.
26. Tschop J, et al. (2008) $\gamma\delta$ T cells mitigate the organ injury and mortality of sepsis. *J Leukocyte Biol* 83:581–588.
27. Jameson JM, Cauvi G, Sharp LL, Witherden DA, Havran WL (2005) $\gamma\delta$ T cell-induced hyaluronan production by epithelial cells regulates inflammation. *J Exp Med* 201:1269–1279.
28. Hecht S, et al. (2002) Studies on the nonmevalonate isoprenoid biosynthetic pathway. Simple methods for preparation of isotope-labeled (E)-1-hydroxy-2-methylbut-2-enyl 4-diphosphate. *Tetrahedron Lett* 43:8929–8933.